

Nonanalyticity of circuit complexity across topological phase transitions

Zijian Xiong,¹ Dao-Xin Yao,^{1,*} and Zhongbo Yan^{1,†}

¹*State Key Laboratory of Optoelectronic Materials and Technologies,
School of Physics, Sun Yat-Sen University, Guangzhou 510275, China*

(Dated: January 22, 2022)

The presence of nonanalyticity in observables is a manifestation of phase transitions. Through the study of two paradigmatic topological models in one and two dimensions, in this work we show that the circuit complexity based on our specific quantification can reveal the occurrence of topological phase transitions, both in and out of equilibrium, by the presence of nonanalyticity. By quenching the system out of equilibrium, we find that the circuit complexity grows linearly or quadratically in the short-time regime if the quench is finished instantaneously or in a finite time, respectively. Notably, we find that for both the sudden quench and the finite-time quench, a topological phase transition in the pre-quench Hamiltonian will be manifested by the presence of nonanalyticity in the first-order or second-order derivative of circuit complexity with respect to time in the short-time regime, and a topological phase transition in the post-quench Hamiltonian will be manifested by the presence of nonanalyticity in the steady value of circuit complexity in the long-time regime. We also show that the increase of dimension does not remove, but only weakens the nonanalyticity of circuit complexity. Our findings can be tested in quantum simulators and cold-atom systems.

I. INTRODUCTION

In the development of physics, concepts from one field sometimes are able to revolutionize the understanding of other fields. Recently, the complexity, which was originally developed in quantum information science to characterize how difficult to prepare one target state from certain reference state[1, 2], has been brought into the fields of holography and black hole physics[3–7]. Among various progresses, the two conjectures, namely “complexity equals volume”[3–5] and “complexity equals action”[6, 7], have attracted particular attention and triggered active investigation of complexity in these fields[8–25], hopefully producing new insights in understanding quantum gravity.

In the study of complexity, its quantification is a central topic[25–29]. According to the original quantum-circuit definition, the complexity (in this context, it is usually dubbed circuit complexity) corresponds to the minimum number of elementary gates required to realize a unitary operator U which transfers the reference state $|\psi_R\rangle$ to the target state $|\psi_T\rangle$, i.e., $|\psi_T\rangle = U|\psi_R\rangle$. As the choice of elementary gates itself has a lot of freedom, the quantification based on this principle is apparently not an easy task. A breakthrough was made by Nielsen and collaborators who provided a geometric interpretation to the circuit complexity[30–32]. Concretely, as a desired unitary operator can be generated by some time-dependent Hamiltonian $H(t)$, they impose a cost function $F[H(t)]$ which defines a Riemannian geometry on the space of unitary operations, then the circuit complexity is shown to correspond to the minimal geodesic length of the Riemannian geometry.

The minimal-geodesic-length quantification makes the circuit complexity be a geometric quantity. In contemporary physics, another geometric quantity of great interest is the so-called topological invariant which mathematically characterizes the global geometric property of a closed manifold. Over the past decades, this concept has been demonstrated to

play a fundamental role in characterizing new phases of matter in condensed matter physics[33–36]. As the topological invariant of a phase is defined in terms of the wave function of ground state or the underlying Hamiltonian, a change of topological invariant (or say topological phase transition) thus indicates a dramatic change of the geometry of the manifold defined by the wave function of ground state or the Hamiltonian. Therefore, it is quite natural to expect that a topological phase transition can also be manifested through the circuit complexity if the reference and target states correspond to two distinct ground states. Very recently, Liu *et al.*[37] did find that both equilibrium and dynamical topological phase transitions in the one-dimensional Kitaev model[38] can be revealed through the circuit complexity. Concretely, they found that by choosing the ground states of the Kitaev model as the reference and target states, the circuit complexity exhibits nonanalytic behavior at the critical points where the target ground state undergoes a dramatic change in topology. In addition, when the Kitaev model undergoes a sudden quench, they found that by choosing the pre-quench ground state as the reference state and the post-quench unitary evolution state as the target state, the circuit complexity first increases and then saturates, with the steady value displaying nonanalyticity when the Kitaev model is quenched across a critical point.

As the cost function itself has some arbitrariness, the quantification of circuit complexity is not unique. It is therefore worthy to find out that whether the nonanalyticity of circuit complexity is preserved or not when a different quantification is adopted. Given this, in this work we consider a cost function distinct from Ref.[37] to quantify the circuit complexity. For generality, we further consider two topological models with richer phase diagrams. As dimension is known to have strong impact on both classical and quantum phase transitions, here we consider that the two topological models take different dimensions to reveal its impact on the circuit complexity. To reveal whether the presence of nonanalyticity in the circuit complexity is generic or not when the

system is quenched out of equilibrium, both sudden quench and finite-time quench are investigated. Our main findings can be summarized as follows: (i) while we adopt a distinct quantification, the presence of nonanalyticity in circuit complexity across topological phase transitions holds. (ii) We find that the long-time behavior of the post-quench circuit complexity is not sensitive to the way of quench. Similarly to Ref.[37], we find that for both the sudden quench and the finite-time quench, the steady value of circuit complexity based on our quantification in the long-time regime can reveal the occurrence of topological phase transitions in the post-quench Hamiltonian by the presence of nonanalyticity. (iii) The short-time growth behavior of the post-quench circuit complexity, however, is found to depend on the way of quench. It grows linearly/quadratically with time for the sudden/finite-time quench in the short-time regime. Notably, we find that the first-order (for sudden quench) or second-order (for finite-time quench) derivative of circuit complexity with respect to time in this regime can reveal the occurrence of topological phase transitions in the pre-quench Hamiltonian by the presence of nonanalyticity. It is noteworthy that unlike the steady value, the determination of the short-time growth behavior can be done very quickly since it requires very little information in the short-time regime, therefore, we believe that this finding is particularly useful for the experimental study of topological phase transitions. (iv) We find that the increase of dimension does not remove, but only weakens the nonanalyticity of circuit complexity, demonstrating the generality of the underlying physics. As in recent years equilibrium and dynamical topological phase transitions are of great interest both in theory[39–53] and in experiment[54–58], our findings may shed new light on this active field.

The paper is organized as follows. In Sec.II, we introduce our quantification of circuit complexity and show that across various topological phase transitions in one dimension, the circuit complexity always displays nonanalyticity at the critical points. In Sec.III, we consider that the one-dimensional generalized Kitaev model is suddenly quenched. We study the evolution of circuit complexity after the sudden quench and show that the short-time and long-time behavior of the post-quench circuit complexity can respectively reveal the occurrence of topological phase transitions in the pre-quench and post-quench Hamiltonian. In Sec.IV, we consider that the quench process is finished in a finite time and show that the conclusions for the sudden quench are preserved. In Sec.V, we generalize the study to two dimensions and discuss the impact of dimension on the circuit complexity. We conclude in Sec.VI. Some calculation details are relegated to appendices.

II. CIRCUIT COMPLEXITY AND TOPOLOGICAL PHASE TRANSITIONS IN ONE DIMENSION

We start with a generalized Kitaev model which takes the form $H = \frac{1}{2} \sum_k \psi_k^\dagger H(k) \psi_k$ with $\psi_k = (c_k, c_{-k}^\dagger)^T$ and $H(k) = (-t_1 \cos k - t_2 \cos 2k - \mu)\tau_z + (\Delta_1 \sin k + \Delta_2 \sin 2k)\tau_y$

$$\equiv d_z(k)\tau_z + d_y(k)\tau_y, \quad (1)$$

where $\tau_{x,y,z}$ are Pauli matrices in particle-hole space, t_1 (Δ_1) and t_2 (Δ_2) represents the nearest-neighbor and next-nearest-neighbor hopping (pairing) amplitude, respectively, and μ is the chemical potential. For convenience, the lattice constant is set to unit throughout this work.

Owing to the presence of chiral symmetry, i.e., $\{\tau_x, H(k)\} = 0$, this model belongs to the class BDI[59–61] and is known to be characterized by the winding number defined as[61]

$$\nu = \frac{i}{4\pi} \int_{-\pi}^{\pi} dk \text{Tr}[\tau_x H^{-1}(k) \partial_k H(k)]. \quad (2)$$

According to the above formula, we present the phase diagram corresponding to $\Delta_1 = \Delta_2 \neq 0$ in Fig.1(a). Noteworthily, as a topological phase transition is associated with the closure of bulk energy gap, the phase boundaries in the phase diagram can be easily determined, which are found to be the lines satisfying $\mu = t_1 - t_2$, $\mu = -t_1 - t_2$ and $\mu = (t_1 + t_2)/2$. In comparison to the standard Kitaev model which only involves the nearest-neighbor hopping and pairing [38], it is readily seen that the presence of additional next-nearest-neighbor hopping and pairing leads to a richer phase diagram, and therefore more topological phase transitions can be investigated to demonstrate the generality of the presence of nonanalyticity in circuit complexity.

The generalized Kitaev model above describes a spinless superconductor. By following the standard Bogoliubov transformation, the model can be diagonalized and accordingly the ground-state wave function can be obtained, which reads[62]

$$|\Omega\rangle = \prod_{k>0} |\psi_k\rangle = \prod_{k>0} (\cos(\theta_k/2) + i \sin(\theta_k/2) c_k^\dagger c_{-k}^\dagger) |0\rangle, \quad (3)$$

where $\theta_k = \arctan(d_y(k)/d_z(k))$. As here the momentum is a good quantum number, we can treat each k independently[37]. For each k , one can see that the state is a superposition of $|0\rangle$ and $c_k^\dagger c_{-k}^\dagger |0\rangle$, and the superposition is characterized by a single parameter $\theta_k/2$ (noteworthily, $\theta_k/2$ and $\theta_k/2 + \pi$ are equivalent as the π difference only results in a global phase difference to the wave function). Taking the ground state with $\theta_k^R/2$ and $\theta_k^T/2$ as the reference state $|\psi_k^R\rangle$ and target state $|\psi_k^T\rangle$, respectively, then the effect of unitary operator is equivalent to doing a transport from the point $\theta_k^R/2$ to the point $\theta_k^T/2$ on the unit circle. Apparently, on the circle the length of the arc connecting $\theta_k^R/2$ and $\theta_k^T/2$ provides a natural measure of the distance between the two states. Owing to the equivalence between $\theta_k/2$ and $\theta_k/2 + \pi$, the minimal length of the arc is in fact given by $\arccos |\langle \psi_k^T | \psi_k^R \rangle|$, where $|\langle \psi_k^T | \psi_k^R \rangle|$ is known as fidelity. In fact, such a quantification corresponds to the well-known quantification of circuit complexity in terms of inner-product metric[62, 63]. Throughout this work, we adopt this quantification which has a simple and clear geometric interpretation.

Accordingly, if we start with a ground state $|\Omega^R\rangle$ and adiabatically transfer it to another ground state $|\Omega^T\rangle$, then the corresponding circuit complexity is

$$C = \sum_{k>0} \arccos |\langle \psi_k^T | \psi_k^R \rangle| = \sum_{k>0} \arccos |\cos(\Delta\theta_k/2)|, \quad (4)$$

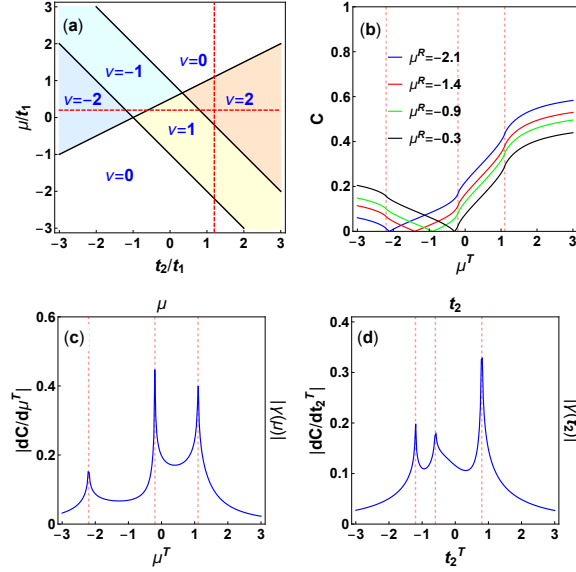


FIG. 1. (Color online) (a) Phase diagram. ν denotes the winding number, and the horizontal ($\mu/t_1=0.2$) and vertical ($t_2/t_1 = 1.2$) red dashed lines are two paths that we choose to vary the parameters. (b) Circuit complexity (in units of system size, below this is implicitly assumed) for several reference states. Parameters are $t_1 = 1$, $t_2 = 1.2$, and $\Delta_1 = \Delta_2 = 1$. (c) The derivative of circuit complexity with respect to μ^T . Parameters are the same as in (b). $|dC/d\mu^T|$ turns out to be independent of μ^R , and is equal to $\gamma(\mu)$. (d) The derivative of circuit complexity with respect to t_2^T . Parameters are $t_1 = 1$, $\mu = 0.2$, and $\Delta_1 = \Delta_2 = 1$. $|dC/dt_2^T|$ is also found to be independent of t_2^R and coincide with $\gamma(t_2)$. Throughout this work, vertical pink dashed lines (see (b)(c)(d)) correspond to the critical points at which topological phase transitions take place.

where $\Delta\theta_k = \theta_k^T - \theta_k^R$. For each k , one can see that the maximum value is $\pi/2$, which corresponds to that $|\psi_k^R\rangle$ and $|\psi_k^T\rangle$ are orthogonal. For comparison, the formula for circuit complexity in Ref.[37] takes the form $C = \sum_k (\Delta\theta_k/2)^2$. While in essence the two formulas only differ by a square-root operation, in the following one will see that remarkable differences will arise in the behaviors of circuit complexity. To simplify the analysis of circuit complexity, below we will restrict ourselves to ground state evolutions corresponding to the variation of only one parameter of the model. Concretely, we will fix $(t_1, \Delta_1, \Delta_2)$ and only vary either μ or t_2 .

In Fig.1(b), we present the circuit complexity associated with the variation of μ . The result clearly demonstrates the presence of nonanalyticity in the C - μ^T curve. The nonanalytic behavior becomes even more apparent by performing a first-order derivative, i.e., $dC/d\mu^T$. As shown in Fig.1(c), divergence appears exactly at the critical points of topological phase transitions. Furthermore, it is readily found that in Fig.1(c) $dC/d\mu^T$ does not depend on μ^R , that is, the first-order derivative of circuit complexity does not depend on the choice of reference state. Noteworthily, such an independence of reference state is absent in Ref.[37], indicating that different quantifications may lead to remarkable different behaviors in the circuit complexity.

Let us now give a simple explanation of the presence of nonanalyticity. For this generalized Kitaev model, its topological invariant, the winding number, characterizes the number of times that the vector $\mathbf{d}(\mathbf{k}) = (d_y(\mathbf{k}), d_z(\mathbf{k}))$ winds around the origin when k goes from $-\pi$ to π . When a topological phase transition occurs, the number of times that the vector $\mathbf{d}(\mathbf{k})$ winds around the origin has a discrete change. Accordingly, the angle θ_k , which characterizes the orientation of the vector $\mathbf{d}(\mathbf{k})$, must jump at some k . Apparently, $\Delta\theta_k$ for these k also jump at the critical points. Then according to Eq.(4), it is readily seen that the circuit complexity will be nonanalytic at the critical points.

Before proceeding, here we define a quantity,

$$\gamma(\lambda) \equiv \sum_{k>0} \lim_{\delta\lambda \rightarrow 0^+} \frac{\arccos |\langle \psi_k(\lambda + \delta\lambda) | \psi_k(\lambda) \rangle|}{\delta\lambda}, \quad (5)$$

where λ denotes some parameter of the Hamiltonian. The physical meaning of this quantity is quite obvious. It characterizes the growth rate of circuit complexity when a state is adiabatically transferred to its nearby state. For the sake of discussion convenience, we name it *adiabatical growth rate*. According to Eq.(3), a short calculation reveals[62]

$$\gamma(\lambda) = \sum_{k>0} \frac{1}{2} \left| \frac{d\theta_k}{d\lambda} \right|. \quad (6)$$

As mentioned above, when a topological phase transition occurs, $\Delta\theta_k$ will dramatically change for some k . Therefore, it is quite obvious that $\gamma(\lambda)$ is also nonanalytic at the critical points. Interestingly, we find that $|dC/d\mu^T|$ and $\gamma(\mu)$ coincide with each other, as shown in Fig.1(c). The divergence of $\gamma(\mu)$ at the critical points indicates that the adiabatical growth rate goes divergent when the state gets close to a critical point. In other words, when the reference state gets more close to a critical point, it becomes more difficult to prepare the target state in an adiabatical way. Noteworthily, the overlap of the adiabatical growth rate and the first-order derivative is not accidental. As shown in Fig.1(d), it also appears when we fix μ and vary t_2 . This overlap is apparently related to the result that the first-order derivative of circuit complexity is independent of the reference state, indicating that this property is tied to our quantification.

III. SUDDEN QUENCH AND CIRCUIT COMPLEXITY EVOLUTION

In equilibrium, as the Hamiltonian and the ground state are tied to each other, the topological invariants defined in terms of them are equivalent. When out of equilibrium, however, as the underlying instantaneous wave function in general does not correspond to the ground state of the instantaneous Hamiltonian, the topological invariants defined in terms of instantaneous Hamiltonian (labeled as ν_H) and instantaneous wave function (labeled as ν_w) are not guaranteed to be equivalent. In particular, when a system is isolated from the environment,

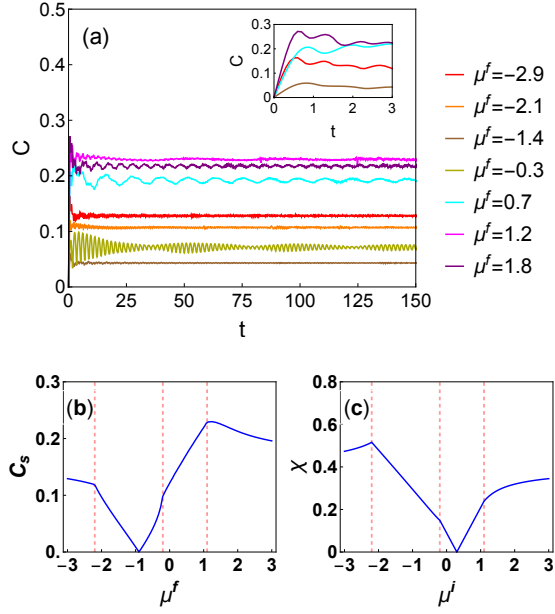


FIG. 2. (Color online) Common parameters are $t_1 = 1$, $t_2 = 1.2$, and $\Delta_1 = \Delta_2 = 1$. (a) The evolution of post-quench circuit complexity. $\mu^i = -0.9$. (b) Steady value of post-quench circuit complexity shown in (a). (c) Dynamical growth rate. $\mu^f = 0.3$ is fixed.

the wave function will follow unitary evolution, and so v_w will keep its value no matter how v_H changes[64, 65]. Therefore, for an isolated system out of equilibrium, a topological phase transition can only be defined as a change of v_H . As out of equilibrium, transitions associated with a change of v_H are usually dubbed dynamical topological phase transitions. In the following, we focus on such isolated systems and first investigate the evolution of circuit complexity after a sudden quench[66–73].

For concreteness, we consider that for $t < 0$, the system is described by H_i and stays at its ground state $|\Omega^i\rangle$. At $t = 0$, the Hamiltonian is suddenly quenched to H_f , and afterwards it keeps as H_f . Accordingly, the wave function at $t > 0$ is given by $|\Omega(t)\rangle = e^{-iH_f t}|\Omega^i\rangle$. For each k , we have $|\psi_k(t)\rangle = e^{-iH_f(k)t}|\psi_k^i\rangle$. Thus, the post-quench circuit complexity is given by $C(t) = \sum_{k>0} \arccos |\langle \psi_k(t) | \psi_k^i \rangle|$. A short calculation reveals[62]

$$C(t) = \sum_{k>0} \arccos \sqrt{1 - \sin^2 \Delta \tilde{\theta}_k \sin^2(E_f(k)t)}, \quad (7)$$

where $\Delta \tilde{\theta} = \theta_k^f - \theta_k^i$ with $\theta_k^{f(i)} = \arctan(d_y^{f(i)}(k)/d_z^{f(i)}(k))$, and $E_f(k) = \sqrt{(d_y^f(k))^2 + (d_z^f(k))^2}$.

By fixing μ_i , we show the evolution of post-quench circuit complexity for a series of μ_f in Fig.2(a). One can see that after the quench, the circuit complexity will first grow linearly with time (see the inset) and then saturate with some degree of oscillations. While adopting a different quantification, we find that similarly to Ref.[37], here the steady value in the long-time regime also exhibits nonanalyticity at the critical

points where the topology of the post-quench Hamiltonian H_f undergoes a change, as shown in Fig.2(b). Noteworthy, as oscillations always appear, we take the average of $C(t)$ over a sufficiently long time as the steady value. Throughout this work we take $C_s = (\int_{t_i}^{t_f} C(t)dt)/(t_f - t_i)$, with $t_i = 50$ and $t_f = 130$.

From above it is readily seen that obtaining the steady value requires us to know the evolution of $C(t)$ for quite a long time, therefore, using the steady value to detect the occurrence of topological phase transitions is not very efficient. Surprisingly, we find that the growth rate of post-quench circuit complexity within the linear growth regime in fact can also reveal the occurrence of topological phase transitions. In order to distinguish from the equilibrium case, here we name it *dynamical growth rate*. As the circuit complexity grows linearly right after the quench, the dynamical growth rate is thus simply given by

$$\chi \equiv \lim_{\delta t \rightarrow 0^+} \frac{C(\delta t)}{\delta t} = \sum_{k>0} |\sin \Delta \tilde{\theta}_k| E_f(k), \quad (8)$$

or equivalently, $\chi \equiv \partial_t C|_{t \rightarrow 0^+}$. One can see that for each k , the dynamical growth rate is proportional to the energy. If starting from different pre-quench Hamiltonian H_i and quenching to the same H_f (e.g., H_f can be chosen to describe a trivial phase for which hopping and pairing are turned off, i.e., $H_f = -\mu\tau_z$), then as $\Delta \tilde{\theta}_k$ displays distinct winding behavior for H_i with distinct v_H , χ will exhibit nonanalyticity at the critical points where the topology of the pre-quench H_i undergoes a change. In Fig.2(c), we present the result for the case with a fixed μ^f . It is readily seen that nonanalyticity does appear at every critical points.

According to Eq.(8), it is quite obvious that the determination of dynamical growth rate requires very little information right after the quench, therefore using it to reveal the occurrence of topological phase transitions is much more convenient and accurate than using the steady value suggested in Ref.[37]. As a final remark of this section, we point out that the linear growth behavior right after the quench is also specific to our quantification. For comparison, in Ref.[37] the circuit complexity does not grow with time in a linear way right after the quench. For their quantification, the slope of the circuit complexity in the extremely short-time regime is time-dependent, and therefore it is hard to give a sharp definition of dynamical growth rate as here, suggesting that a good choice of the quantification may benefit its application.

IV. FINITE-TIME QUENCH AND CIRCUIT COMPLEXITY EVOLUTION

For the sudden quench, the change from the initial Hamiltonian to the final Hamiltonian is completed instantaneously. In this section we consider finite-time quench for which one of the parameters in the Hamiltonian changes from its initial value at $t \leq 0$ to the final value with a finite speed. To be specific, we focus on the chemical potential and take

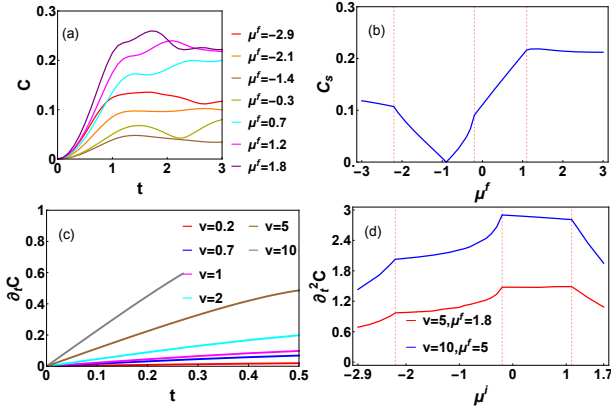


FIG. 3. (a) (Color online) Common parameters are $t_1 = 1$, $t_2 = 1.2$, and $\Delta_1 = \Delta_2 = 1$. (a) The evolution of circuit complexity under a finite-time quench. The quench duration time t_q is fixed to 1 and $\mu^i = -0.9$. (b) The dependence of steady value on μ^f , t_q and μ^i keep the same as in (a). (c) $\partial_t C$, the dynamical growth rate of circuit complexity, in the short-time regime, $\mu^i = -0.9$, $\mu^f = 1.8$. The slope of $\partial_t C$ is found to increase with the quench speed. (d) $\partial_t^2 C$ in the limit $t \rightarrow 0^+$. The concrete value of $\partial_t^2 C$ depends on the quench speed, but the presence of nonanalyticity at the critical points does not rely on the quench speed.

$\mu(t) = \mu^i + v\Theta(t_q - t) + (\mu^f - \mu^i)\Theta(t - t_q)$, where $t_q = |\mu^f - \mu^i|/|v|$ is the quench duration time and $\Theta(x)$ is the step function with $\Theta(x) = 1/0$ for $x > / < 0$. This expression means that the chemical potential is quenched from μ^i to μ^f with a finite speed v . When v goes to infinity, it returns to the sudden quench addressed in the previous section.

As the Hamiltonian changes with time in the domain $0 < t < t_q$, the circuit complexity in this domain is given by

$$C(t) = \sum_{k>0} \arccos |\langle \psi_k^i | T e^{-i \int_0^t H(k,t') dt'} | \psi_k^i \rangle|, \quad (9)$$

where T denotes the time ordering operator. When $t > t_q$,

$$C(t) = \sum_{k>0} \arccos |\langle \psi_k^i | e^{-i H_f(k)(t-t_f)} T e^{-i \int_0^{t_f} H(k,t') dt'} | \psi_k^i \rangle|. \quad (10)$$

By fixing μ^i and t_q , we show the evolution of circuit complexity for a series of μ^f in Fig.3(a). Similarly to the sudden-quench case, we find that the circuit complexity will saturate with some degree of oscillations in the long-time regime (not shown explicitly) and its steady value C_s also displays nonanalyticity at the critical points where the topology of the post-quench Hamiltonian undergoes a change, as shown in Fig.3(b). The similarity in the long-time regime between the sudden quench and the finite-time quench is naturally expected since after t_q the dynamics of the whole system is governed by the same time-independent Hamiltonian H_f for both cases. When looking at the short-time regime in Fig.3(a), we find that the circuit complexity does not grow linearly as in the sudden-quench case. Instead, it grows quadratically with time right after the start of the quench. To better show the quadratic growth, we present the evolution of $\partial_t C$ in Fig.3(c). It is

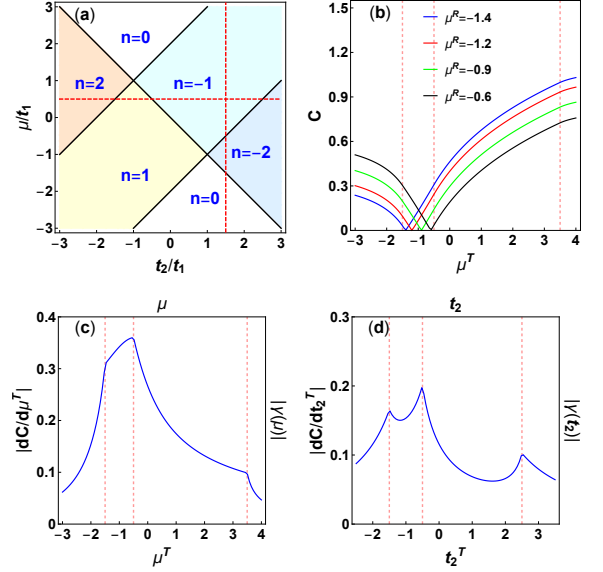


FIG. 4. (a) Phase diagram with n denoting the Chern number. The horizontal ($\mu/t_1 = 0.5$) and vertical ($t_2/t_1 = 1.5$) red dashed lines are two paths that we choose to vary the parameters. (b) Circuit complexity for several reference states. Parameters are $t_1 = 1.0$ and $t_2 = 1.5$. (c) The derivative of circuit complexity with respect to μ^T . Parameters are the same as in (b). (d) The derivative of circuit complexity with respect to t_2^T . Parameters are $t_1 = 1$ and $\mu = 0.5$.

readily seen that right after the start of the quench, $\partial_t C$ grows linearly with time like the circuit complexity after a sudden quench. From Fig.3(c), one can also find that while $\partial_t C$ depends on the quench speed, its linear growth behavior is robust against the variation of the quench speed. The linear growth behavior of $\partial_t C$ leads us to expect that $\partial_t^2 C$, which can be understood as the acceleration of the circuit complexity, will display nonanalyticity at the critical points where the topology of the pre-quench Hamiltonian undergoes a change. The numerical results confirm the above expectation, as shown in Fig.3(d). Therefore, for the finite-time quench, the short-time behavior and the long-time behavior of the circuit complexity can also respectively reveal the occurrence of topological phase transitions in the pre-quench Hamiltonian and in the post-quench Hamiltonian.

V. CIRCUIT COMPLEXITY AND TOPOLOGICAL PHASE TRANSITIONS IN TWO DIMENSIONS

Since a topological phase transition is always associated with a dramatic change of the global geometric property of the underlying ground state wave function or Hamiltonian, it is natural to expect that the circuit complexity will also exhibit nonanalyticity in higher dimensions. To demonstrate this explicitly, here we consider a paradigmatic “ $\mathbf{d} \cdot \boldsymbol{\tau}$ ” model in two dimensions for concreteness. The model reads $H = \frac{1}{2} \sum_{\mathbf{k}} \psi_{\mathbf{k}}^\dagger H(\mathbf{k}) \psi_{\mathbf{k}}$, with $H(\mathbf{k}) = \mathbf{d}(\mathbf{k}) \cdot \boldsymbol{\tau}$ and [52]

$$d_x(\mathbf{k}) = \sin k_x, \quad d_y = -\sin k_y,$$

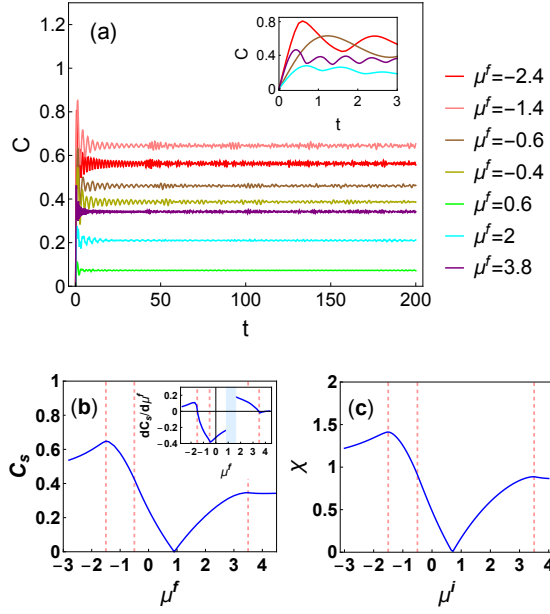


FIG. 5. Common parameters are $t_1 = 1$, $t_2 = 1.5$. (a) The evolution of post-quench circuit complexity. $\mu^i = 0.9$. (b) Steady value of post-quench circuit complexity shown in (a). (c) Dynamical growth rate. $\mu^f = 0.7$ is fixed.

$$d_z(\mathbf{k}) = t_1(\cos k_x + \cos k_y) + t_2 \cos k_x \cos k_y - \mu, \quad (11)$$

where the d_x and d_y terms together describe a chiral p -wave pairing, and the d_z term is the kinetic energy of normal state. As for this Hamiltonian only particle-hole symmetry is preserved, it belongs to the class D that in two dimensions is characterized by the first-class Chern number,

$$n = \frac{1}{4\pi} \int_{BZ} d^2k \hat{\mathbf{d}}(\mathbf{k}) \cdot (\partial_{k_x} \hat{\mathbf{d}}(\mathbf{k}) \times \partial_{k_y} \hat{\mathbf{d}}(\mathbf{k})), \quad (12)$$

where $\hat{\mathbf{d}} = (d_x, d_y, d_z) / \sqrt{d_x^2 + d_y^2 + d_z^2}$. The geometric meaning of this formula also has a winding interpretation: it counts the number of times that the three-component vector $\mathbf{d}(\mathbf{k})$ winds around the origin when the momentum transverses the whole first Brillouin zone. It indicates that when a topological phase transition takes place, the orientation of the vector $\mathbf{d}(\mathbf{k})$ will also change dramatically at some momenta. By using the above formula, we present the phase diagram in Fig. 4(a).

Following the steps in one dimension, we find that for an adiabatical evolution of ground states, the circuit complexity is

$$C = \sum_{k_x > 0, k_y} \arccos |\cos(\Delta\theta_k/2)|, \quad (13)$$

where $\Delta\theta_k$ takes the same definition as in Eq. (4), but here $\theta_k^{T(R)} = \arctan(\sqrt{(d_x^{T(R)}(\mathbf{k}))^2 + (d_y^{T(R)}(\mathbf{k}))^2} / d_z^{T(R)}(\mathbf{k}))$. As for this model all topological phase transitions occur at the time-reversal invariant momenta, including $(k_x, k_y) = (0, 0)$, $(0, \pi)$, $(\pi, 0)$, and (π, π) , at which $d_x(\mathbf{k})$ and $d_y(\mathbf{k})$ vanish identically, it is readily seen that across a critical point, the orientation

of the vector $\mathbf{d}(\mathbf{k})$ will reverse its direction at the respective momenta. Then according to Eq. (13), it is clear that nonanalyticity will also be present in the circuit complexity.

Similarly to the one-dimensional model, in the following we also consider that only μ and t_2 are variables. In Fig. 4(b), we fix t_2 and present several C - μ^T curves corresponding to different μ^R . In comparison to Fig. 1(b), it is readily seen that the increase of dimension enhances the smoothness of the C - μ^T curve. Nevertheless, it is as expected that the circuit complexity also exhibits nonanalyticity at all critical points, and this feature becomes quite obvious after performing a first-order derivative, as shown in Fig. 4(c), where one can see that the overlap of $|dC/d\mu^T|$ and $\gamma(\mu)$ also holds. If fixing μ and varying t_2 , the results also demonstrate the presence of nonanalyticity at the critical points and the overlap of $|dC/dt_2^T|$ and $\gamma(t_2)$, as shown in Fig. 4(d).

The evolution of circuit complexity after a sudden quench is presented in Fig. 5(a). It is readily seen that the long-time and short-time behaviors are quite similar to those in one dimension. Due to this similarity, here we will not discuss the more complicated finite-time quench. From Fig. 5(b)(c), one can find that owing to the increase of dimension, the C_s - μ^f curve, as well as the χ - μ^f curve both become somewhat smoother. Nevertheless, the nonanalyticity at the critical points holds and can be revealed by performing a first-order derivative (see the inset in Fig. 5(b)).

Through Fig. 4 and Fig. 5, we demonstrate that the circuit complexity can also reveal the occurrence of topological phase transitions in higher dimensions. However, as the increase of dimension is shown to weaken the nonanalyticity, it indicates that the application of this quantity to detect higher dimensional topological phase transitions requires a higher precision of measurements.

VI. CONCLUSIONS

In this work, we have adopted a simple quantification of the circuit complexity distinct from Ref. [37] and demonstrated that it can reveal the occurrence of topological phase transitions by the presence of nonanalyticity. By studying the evolution of circuit complexity after a quench, either sudden or finite-time, we find that the growth behavior in the short-time regime and the steady value in the long-time regime can respectively reveal the occurrence of topological phase transitions in the pre-quench Hamiltonian and in the post-quench Hamiltonian by the presence of nonanalyticity. Since the growth behavior in the short-time regime can be determined by very few measurements, its nonanalytic behavior is expected to be very useful for the experimental study of topological phase transitions. Furthermore, we have investigated the effect of dimension and shown that the increase of dimension does not remove, but only weakens the nonanalyticity. As the circuit complexity based on our quantification can be determined by measuring the fidelity, the test of our predictions is well with the current experimental accessibility. For

instance, the two-band models studied can be simulated in a superconducting qubit, and the evolution of states can be measured by performing quantum state tomography[74]. In light of the active study of equilibrium and dynamical topological phase transitions in quantum simulators and cold-atom systems[54–58], our predictions can also be tested in these platforms, hopefully providing some new insights into understanding various phase transitions.

ACKNOWLEDGEMENTS

We would like to acknowledge helpful discussions with Chengfeng Cai. Z.X. and D.X.Y. are supported by NKRDPC Grants No. 2017YFA0206203, No. 2018YFA0306001, NSFC-11574404, NSFG-2015A030313176, National Supercomputer Center in Guangzhou, and Leading Talent Program of Guangdong Special Projects. Z.Y. would like to acknowledge the support by Startup Grant (No. 74130-18841219) and NSFC-11904417.

Appendix A: Derivation of the circuit complexity under the inner-product metric

As mentioned in the main text, $|\psi_k\rangle$ is a superposition of $|0\rangle$ and $c_k^\dagger c_{-k}^\dagger |0\rangle$. Therefore, under the basis $(c_k^\dagger c_{-k}^\dagger |0\rangle, |0\rangle)$, $|\psi_k\rangle$ can be written as a two-component spinor,

$$|\psi_k\rangle = \begin{pmatrix} i \sin(\theta_k/2) \\ \cos(\theta_k/2) \end{pmatrix}. \quad (14)$$

A two-component spinor can be mapped to a three-component vector in terms of the Pauli matrices,

$$\psi_k = \langle \psi_k | \sigma | \psi_k \rangle = -(0, \sin \theta_k, \cos \theta_k)^T. \quad (15)$$

Let us consider that the target state is infinitely close to the reference state, i.e., $|\psi^R\rangle = |\psi_k\rangle$, and $|\psi^T\rangle = |\psi_k + d\psi_k\rangle$, or equivalently, $\psi^R = \psi_k$, and $\psi^T = \psi_k + d\psi_k$. The normalization requires $\psi_k \cdot d\psi_k = 0$. As the two states are infinitely close to each other, to leading order, the unitary operator which transforms the reference state to the target state can be written as

$$U = \mathbf{I} + i\mathbf{F}(\psi_k) \cdot \sigma + \dots \quad (16)$$

where $\mathbf{F}(\psi_k)$ is an infinitely small parameter to be determined. As $|\psi^T\rangle = U|\psi^R\rangle$ and $\psi^T = \psi_k + d\psi_k = \langle \psi^T | \sigma | \psi^T \rangle$, it is readily found that to leading order of $\mathbf{F}(\psi_k)$.

$$\begin{aligned} d\psi_k &= i\langle \psi_k | (\sigma \mathbf{F}(\psi_k) \cdot \sigma - \mathbf{F}(\psi_k) \cdot \sigma \sigma) | \psi_k \rangle \\ &= -2\langle \psi_k | \mathbf{F}(\psi_k) \times \sigma | \psi_k \rangle. \end{aligned} \quad (17)$$

A solution of the above equation is

$$\mathbf{F}(\psi_k) = \frac{1}{2}(d\psi_k \times \psi_k + \alpha \psi_k), \quad (18)$$

where α denotes an infinitely small constant. Therefore, to leading order, the unitary operator for an infinitely small change of the state is given by

$$U = \mathbf{I} + \frac{i}{2}(d\psi_k \times \psi_k + \alpha \psi_k) \cdot \sigma. \quad (19)$$

Ignoring global phase, U belongs to the $SU(2)$ group. The standard inner-product metric on $SU(2)$ is[63]

$$\begin{aligned} ds^2 &= \frac{1}{2} \text{Tr}[dU^\dagger dU] \\ &= \frac{(d\psi_k \times \psi_k + \alpha \psi_k) \cdot (d\psi_k \times \psi_k + \alpha \psi_k)}{4} \\ &= \frac{d\psi_k \cdot d\psi_k + \alpha^2}{4}, \end{aligned} \quad (20)$$

which is minimized when $\alpha = 0$. Accordingly, the inner-product metric is $ds^2 = d\psi_k \cdot d\psi_k/4 = d\theta_k^2/4$. Therefore, the circuit complexity, which corresponds to the geodesic length, is given by

$$ds = |d\theta_k|/2 = \arccos |\langle \psi_k + d\psi_k | \psi_k \rangle|. \quad (21)$$

Above we have used that

$$|\psi_k + d\psi_k\rangle = \begin{pmatrix} i \sin((\theta_k + d\theta_k)/2) \\ \cos((\theta_k + d\theta_k)/2) \end{pmatrix}. \quad (22)$$

Performing a summation over k , we reach the expression of circuit complexity in Eq.(4) of the main text.

Appendix B: The wave function of ground state

We start with the Hamiltonian $H = \frac{1}{2} \sum_k \psi_k^\dagger H(k) \psi_k$ with $\psi_k = (c_k, c_{-k}^\dagger)^T$ and

$$\begin{aligned} H(k) &= (-t_1 \cos k - t_2 \cos 2k - \mu)\tau_z + (\Delta_1 \sin k + \Delta_2 \sin 2k)\tau_y \\ &\equiv d_z(k)\tau_z + d_y(k)\tau_y. \end{aligned} \quad (23)$$

By performing a standard Bogoliubov transformation, i.e.,

$$\begin{aligned} c_k &= \cos \frac{\theta_k}{2} \alpha_k + i \sin \frac{\theta_k}{2} \alpha_{-k}^\dagger, \\ c_{-k}^\dagger &= i \sin \frac{\theta_k}{2} \alpha_k + \cos \frac{\theta_k}{2} \alpha_{-k}^\dagger, \end{aligned} \quad (24)$$

where $\theta_k = \arctan(d_y(k)/d_z(k))$, the Hamiltonian will be diagonalized as

$$\begin{aligned} H &= \frac{1}{2} \sum_k E_k (\alpha_k^\dagger \alpha_k - \alpha_{-k}^\dagger \alpha_{-k}) \\ &= \sum_{k>0} E_k (\alpha_k^\dagger \alpha_k + \alpha_{-k}^\dagger \alpha_{-k}) + \dots, \end{aligned} \quad (25)$$

where “...” stands for some unimportant constant, and $E_k = \sqrt{d_y^2(k) + d_z^2(k)}$. The ground state satisfies $\alpha_k |\Omega\rangle = 0$ for arbitrary k . One can find that the solution is

$$|\Omega\rangle = \prod_{k>0} |\psi_k\rangle = \prod_{k>0} (\cos \frac{\theta_k}{2} + i \sin \frac{\theta_k}{2} c_k^\dagger c_{-k}^\dagger) |0\rangle, \quad (26)$$

where $|0\rangle$ represents the vacuum, i.e., $c_k|0\rangle = 0$. As k is a good quantum number, we can treat each k independently. For each k , $|\psi_k\rangle$ is a superposition of $|0\rangle$ and $c_k^\dagger c_{-k}^\dagger|0\rangle$. Let us focus on a specific k and consider that the reference state is given by $|\psi_k^R\rangle = (\cos \frac{\theta_k^R}{2} + i \sin \frac{\theta_k^R}{2} c_k^\dagger c_{-k}^\dagger)|0\rangle$, and the target state is given by $|\psi_k^T\rangle = (\cos \frac{\theta_k^T}{2} + i \sin \frac{\theta_k^T}{2} c_k^\dagger c_{-k}^\dagger)|0\rangle$. The inner product of the two states, which is also known as fidelity, is given by

$$\begin{aligned} |\langle \psi_k^T | \psi_k^R \rangle| &= |\cos(\theta_k^T/2) \cos(\theta_k^R/2) + \sin(\theta_k^T/2) \sin(\theta_k^R/2)| \\ &= |\cos((\theta_k^T - \theta_k^R)/2)| \\ &= |\cos(\Delta\theta_k/2)|. \end{aligned} \quad (27)$$

Appendix C: The growth rate of adiabatic circuit complexity

Here we give a derivation of Eq.(6) in the main text. Consider a ground state $|\Omega^R\rangle = \prod_{k>0} |\psi_k(\lambda)\rangle$ as the reference state, where λ refers to the parameter to vary, and consider its near neighbour $|\Omega^T\rangle = \prod_{k>0} |\psi_k(\lambda + \delta\lambda)\rangle$ as the target state, then according to Eq.(4) in the main text, we have

$$\delta C(\lambda) = \sum_{k>0} \arccos |\langle \psi_k(\lambda + \delta\lambda) | \psi_k(\lambda) \rangle|. \quad (28)$$

To characterize the growth rate of circuit complexity when λ is adiabatically varied away from its reference state's value, a natural definition of the growth rate is

$$\gamma(\lambda) \equiv \lim_{\delta\lambda \rightarrow 0^+} \frac{\delta C(\lambda)}{\delta\lambda} = \sum_{k>0} \lim_{\delta\lambda \rightarrow 0^+} \frac{\arccos |\langle \psi_k(\lambda + \delta\lambda) | \psi_k(\lambda) \rangle|}{\delta\lambda} \quad (29)$$

As $\delta\lambda$ is infinitely small, it's justified to make a Taylor expansion,

$$\begin{aligned} \langle \psi_k(\lambda + \delta\lambda) | \psi_k(\lambda) \rangle &= \langle \psi_k(\lambda) | \psi_k(\lambda) \rangle + \langle \frac{d\psi_k(\lambda)}{d\lambda} | \psi_k(\lambda) \rangle \delta\lambda \\ &\quad + \frac{1}{2} \langle \frac{d^2\psi_k(\lambda)}{d\lambda^2} | \psi_k(\lambda) \rangle (\delta\lambda)^2 + \dots \end{aligned} \quad (30)$$

According to the expression of $|\psi_k(\lambda)\rangle$, one can easily find that the linear-order term vanishes. Therefore, up to second-order of $\delta\lambda$, we have

$$|\langle \psi_k(\lambda + \delta\lambda) | \psi_k(\lambda) \rangle| = 1 - \frac{1}{8} \left(\frac{d\theta_k}{d\lambda} \right)^2 (\delta\lambda)^2. \quad (31)$$

Accordingly, we have

$$\begin{aligned} \delta C(\lambda) &= \sum_{k>0} \arccos |\langle \psi_k(\lambda + \delta\lambda) | \psi_k(\lambda) \rangle| \\ &= \sum_{k>0} \arccos \left(1 - \frac{1}{8} \left(\frac{d\theta_k(\lambda)}{d\lambda} \right)^2 (\delta\lambda)^2 \right) \\ &= \sum_{k>0} \sqrt{2} \sqrt{\frac{1}{8} \left(\frac{d\theta_k(\lambda)}{d\lambda} \right)^2 (\delta\lambda)^2} + \dots \\ &= \sum_{k>0} \frac{1}{2} \left| \frac{d\theta_k(\lambda)}{d\lambda} \right| \delta\lambda, \end{aligned} \quad (32)$$

and

$$\begin{aligned} \gamma(\lambda) &= \lim_{\delta\lambda \rightarrow 0^+} \frac{\delta C(\lambda)}{\delta\lambda} \\ &= \sum_{k>0} \frac{1}{2} \left| \frac{d\theta_k(\lambda)}{d\lambda} \right|. \end{aligned} \quad (33)$$

To see that $\gamma(\lambda)$ is nonanalytic at critical points, we take a special case of the model in Eq.(23) for illustration. Concretely, we take $t_2 = \Delta_2 = 0$ and $t_1 = \Delta_1 = 1$. Accordingly, we have

$$H(k) = (-\cos k - \mu)\tau_z + \sin k \tau_y. \quad (34)$$

For this Hamiltonian, topological phase transitions take place at $\mu = \pm 1$. As only μ is a variable, we let $\lambda = \mu$, then we have

$$\begin{aligned} \gamma(\mu) &= \sum_{k>0} \frac{1}{2} \left| \frac{d\theta_k(\mu)}{d\mu} \right| \\ &= \frac{1}{2} \sum_{k>0} \frac{\sin k}{(\cos k + \mu)^2 + \sin^2 k} \\ &= \frac{L}{2} \int_0^\pi \frac{dk}{2\pi} \frac{\sin k}{(\cos k + \mu)^2 + \sin^2 k} \\ &= \frac{L}{4\pi} \int_{-1}^1 \frac{dx}{1 + \mu^2 + 2\mu x} \\ &= \frac{L}{4\pi\mu} \ln \left| \frac{1 + \mu}{1 - \mu} \right|, \end{aligned} \quad (35)$$

where L denotes the system size. One can see that $\gamma(\mu)$ exhibits logarithmic divergence exactly at the two critical points $\mu = \pm 1$.

According to Eq.(33), one can understand that the presence of divergence in $\gamma(\mu)$ at a critical point is because θ_k will undergo a dramatic change across a topological phase transition. To see this intuitively, we go back to the more general model in Eq.(23) and plot θ_k - k curves near the critical points. As shown in Fig.6, θ_k will undergo a sudden jump at some momenta when the system goes across a topological phase transition. Such sudden jumps lead to the presence of divergence in $\gamma(\mu)$.

Appendix D: Post-quench circuit complexity

In the main text, we have considered a global quench of the Hamiltonian. Concretely, we consider that before quench, the system is described by H_i and stays at its ground state $|\Omega^i\rangle$. At $t = 0$, the underlying Hamiltonian is suddenly quenched to H_f , and afterwards it keeps as H_f . For an isolated system, the wave function follows a unitary evolution, i.e., $|\Omega(t)\rangle = e^{-iH_f t} |\Omega^i\rangle$ for $t > 0$. For each k , we have $|\psi_k(t)\rangle = e^{-iH_f(k)t} |\psi_k^i\rangle$. Thus, the post-quench circuit complexity is given by $C(t) = \sum_{k>0} \arccos |\langle \psi_k(t) | \psi_k^i \rangle|$.

To obtain the concrete expression of $C(t)$, we need to know $|\psi_k(t)\rangle$. According to the unitary evolution,

$$\begin{aligned} |\psi_k(t)\rangle &= e^{-iH_f(k)t} |\psi_k^i\rangle \\ &= e^{iE_f(k)t} \langle \psi_{k,-}^f | \psi_k^i \rangle |\psi_{k,-}^f\rangle + e^{-iE_f(k)t} \langle \psi_{k,+}^f | \psi_k^i \rangle |\psi_{k,+}^f\rangle, \end{aligned}$$

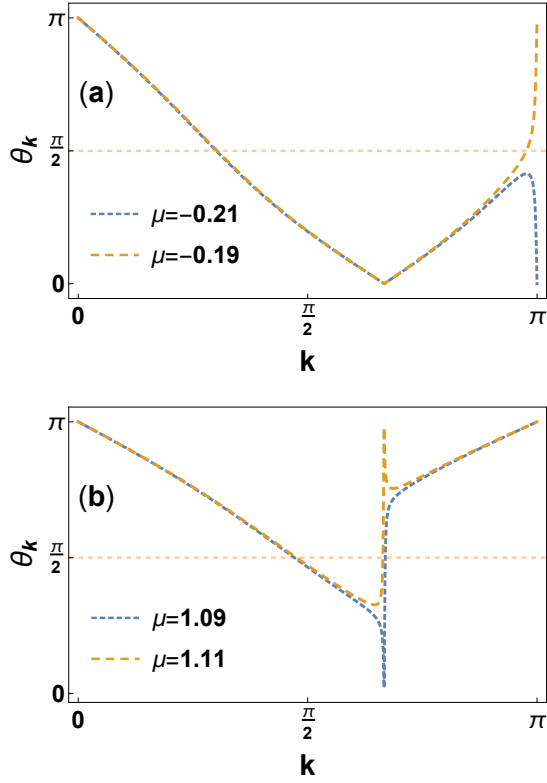


FIG. 6. θ_k - k curves near critical points. Common parameters are $t_1 = 1$, $t_2 = 1.2$, and $\Delta_1 = \Delta_2 = 1$. (a) Across the critical point $\mu_c = -0.2$, one can see that θ_k has a sudden jump at $k = \pi$. (b) Across the critical point $\mu_c = 1.1$, θ_k has a sudden jump at $k = 2\pi/3$.

(36)

where $|\psi_{k,\pm}^f\rangle$ are the eigenstates of $H_f(k)$, with $|\psi_{k,+}^f\rangle$ and $|\psi_{k,-}^f\rangle$ corresponding to eigenenergy $E_f(k)$ and $-E_f(k)$, respectively.

Here $E_f(k) = \sqrt{(d_y^f(k))^2 + (d_z^f(k))^2}$. According to Eq.(26), one has

$$\begin{aligned} |\psi_{k,-}^f\rangle &= (\cos \frac{\theta_k^f}{2} + i \sin \frac{\theta_k^f}{2} c_k^\dagger c_{-k}^\dagger) |0\rangle, \\ |\psi_{k,+}^f\rangle &= (i \sin \frac{\theta_k^f}{2} + \cos \frac{\theta_k^f}{2} c_k^\dagger c_{-k}^\dagger) |0\rangle, \end{aligned} \quad (37)$$

then a short calculation reveals

$$\begin{aligned} \langle \psi_k(t) | \psi_k^i \rangle &= e^{-iE_f(k)t} \langle \psi_{k,-}^f | \psi_k^i \rangle \langle \psi_k^i | \psi_{k,-}^f \rangle \\ &\quad + e^{iE_f(k)t} \langle \psi_{k,+}^f | \psi_k^i \rangle \langle \psi_k^i | \psi_{k,+}^f \rangle \\ &= e^{-iE_f(k)t} \cos^2 \frac{\Delta\theta_k}{2} + e^{iE_f(k)t} \sin^2 \frac{\Delta\theta_k}{2}, \end{aligned} \quad (38)$$

where $\Delta\theta_k = \theta_k^f - \theta_k^i$. Therefore,

$$\begin{aligned} |\langle \psi_k(t) | \psi_k^i \rangle| &= \sqrt{\cos^2(E_f(k)t) + \cos^2 \Delta\theta_k \sin^2(E_f(k)t)} \\ &= \sqrt{1 - \sin^2 \Delta\theta_k \sin^2(E_f(k)t)}. \end{aligned} \quad (39)$$

Accordingly, we obtain the expression for post-quench circuit complexity,

$$C(t) = \sum_{k>0} \arccos \sqrt{1 - \sin^2 \Delta\theta_k \sin^2(E_f(k)t)}. \quad (40)$$

Appendix E: Growth rate of post-quench circuit complexity

In the main text, we have shown that right after the quench, the post-quench circuit complexity grows linearly with time. As the slope of a line can be determined by any two points on the line, thus the growth rate of post-quench circuit complexity can be defined as

$$\chi \equiv \lim_{\delta t \rightarrow 0^+} \frac{C(\delta t) - C(0)}{\delta t} = \lim_{\delta t \rightarrow 0^+} \frac{C(\delta t)}{\delta t}. \quad (41)$$

Above we have used $C(0) = 0$. According to Eq.(40), we have

$$\begin{aligned} \chi &= \sum_{k>0} \lim_{\delta t \rightarrow 0^+} \frac{\arccos \sqrt{1 - \sin^2 \Delta\theta_k \sin^2(E_f(k)\delta t)}}{\delta t} \\ &= \sum_{k>0} \lim_{\delta t \rightarrow 0^+} \frac{\arccos(1 - \frac{1}{2} \sin^2 \Delta\theta_k (E_f(k)\delta t)^2 + O((\delta t)^3))}{\delta t} \\ &= \sum_{k>0} \lim_{\delta t \rightarrow 0^+} \frac{\sqrt{2} \sqrt{\frac{1}{2} \sin^2 \Delta\theta_k (E_f(k)\delta t)^2 + O((\delta t)^3)}}{\delta t} \\ &= \sum_{k>0} |\sin \Delta\theta_k| E_f(k). \end{aligned} \quad (42)$$

To see that χ is nonanalytic at the critical points, we again consider the special model in Eq.(34) for illustration. Concretely, we consider

$$\begin{aligned} H_i(k) &= (-\cos k - \mu^i) \tau_z + \sin k \tau_y, \\ H_f(k) &= -\mu^f \tau_z. \end{aligned} \quad (43)$$

Accordingly, we have

$$\begin{aligned} \chi &= \sum_{k>0} |\sin \Delta\theta_k| E_f(k) \\ &= \sum_{k>0} \frac{\sin k}{\sqrt{(\cos k + \mu^i)^2 + \sin^2 k}} |\mu^f| \\ &= \frac{L|\mu^f|}{2\pi} \int_0^\pi dk \frac{\sin k}{\sqrt{(\cos k + \mu^i)^2 + \sin^2 k}} \\ &= \frac{L|\mu^f|}{2\pi} \int_{-1}^1 \frac{dx}{\sqrt{1 + (\mu^i)^2 + 2\mu^i x}} \\ &= \frac{L|\mu^f|}{2\pi} \frac{|1 + \mu^i| - |1 - \mu^i|}{2\mu^i}, \\ &= \begin{cases} \frac{L|\mu^f|}{2\pi}, & |\mu^i| \leq 1, \\ \frac{L|\mu^f|}{2\pi|\mu^i|}, & |\mu^i| > 1. \end{cases} \end{aligned} \quad (44)$$

The nonanalyticity of χ at the two critical points $\mu^i = \pm 1$ is obvious.

* yaodaox@mail.sysu.edu.cn

† yanzhb5@mail.sysu.edu.cn

- [1] C. H. Papadimitriou, *Computational complexity* (John Wiley and Sons Ltd., 2003).
- [2] S. Arora and B. Barak, *Computational complexity: a modern approach* (Cambridge University Press, 2009).
- [3] L. Susskind, *Fortschritte der Physik* **64**, 24 (2016).
- [4] L. Susskind, *Fortschritte der Physik* **64**, 44 (2016).
- [5] D. Stanford and L. Susskind, *Phys. Rev. D* **90**, 126007 (2014).
- [6] A. R. Brown, D. A. Roberts, L. Susskind, B. Swingle, and Y. Zhao, *Phys. Rev. Lett.* **116**, 191301 (2016).
- [7] A. R. Brown, D. A. Roberts, L. Susskind, B. Swingle, and Y. Zhao, *Phys. Rev. D* **93**, 086006 (2016).
- [8] M. Alishahiha, *Phys. Rev. D* **92**, 126009 (2015).
- [9] J. L. F. Barbón and E. Rabinovici, *Journal of High Energy Physics* **2016**, 84 (2016).
- [10] L. Lehner, R. C. Myers, E. Poisson, and R. D. Sorkin, *Phys. Rev. D* **94**, 084046 (2016).
- [11] O. Ben-Ami and D. Carmi, *Journal of High Energy Physics* **2016**, 129 (2016).
- [12] D. Carmi, R. C. Myers, and P. Rath, *Journal of High Energy Physics* **2017**, 118 (2017).
- [13] S. Chapman, H. Marrochio, and R. C. Myers, *Journal of High Energy Physics* **2017**, 62 (2017).
- [14] P. Caputa, N. Kundu, M. Miyaji, T. Takayanagi, and K. Watanabe, *Journal of High Energy Physics* **2017**, 97 (2017).
- [15] P. A. Cano, R. A. Hennigar, and H. Marrochio, *Phys. Rev. Lett.* **121**, 121602 (2018).
- [16] Z. Fu, A. Maloney, D. Marolf, H. Maxfield, and Z. Wang, *Journal of High Energy Physics* **2018**, 72 (2018).
- [17] B. Swingle and Y. Wang, *Journal of High Energy Physics* **2018**, 106 (2018).
- [18] J. Couch, S. Eccles, T. Jacobson, and P. Nguyen, *Journal of High Energy Physics* **2018**, 44 (2018).
- [19] A. R. Brown and L. Susskind, *Phys. Rev. D* **97**, 086015 (2018).
- [20] K. Goto, H. Marrochio, R. C. Myers, L. Queimada, and B. Yoshida, *Journal of High Energy Physics* **2019**, 160 (2019).
- [21] A. R. Brown, H. Gharibyan, H. W. Lin, L. Susskind, L. Thorlacius, and Y. Zhao, *Phys. Rev. D* **99**, 046016 (2019).
- [22] A. Bernamonti, F. Galli, J. Hernandez, R. C. Myers, S.-M. Ruan, and J. Simón, *Phys. Rev. Lett.* **123**, 081601 (2019).
- [23] P. Caputa and J. M. Magan, *Phys. Rev. Lett.* **122**, 231302 (2019).
- [24] J. Jiang, *Phys. Rev. D* **98**, 086018 (2018).
- [25] S. Chapman, M. P. Heller, H. Marrochio, and F. Pastawski, *Phys. Rev. Lett.* **120**, 121602 (2018).
- [26] R. A. Jefferson and R. C. Myers, *Journal of High Energy Physics* **2017**, 107 (2017).
- [27] L. Hackl and R. C. Myers, *Journal of High Energy Physics* **2018**, 139 (2018).
- [28] H. A. Camargo, M. P. Heller, R. Jefferson, and J. Knaute, *Phys. Rev. Lett.* **123**, 011601 (2019).
- [29] J. Jiang and B.-X. Ge, *Phys. Rev. D* **99**, 126006 (2019).
- [30] M. A. Nielsen, arXiv e-prints, quant-ph/0502070 (2005), [arXiv:quant-ph/0502070 \[quant-ph\]](https://arxiv.org/abs/quant-ph/0502070).
- [31] M. A. Nielsen, M. R. Dowling, M. Gu, and A. C. Doherty, *Science* **311**, 1133 (2006).
- [32] M. R. Dowling and M. A. Nielsen, *Quantum Info. Comput.* **8**, 861 (2008).
- [33] M. Z. Hasan and C. L. Kane, *Rev. Mod. Phys.* **82**, 3045 (2010).
- [34] X.-L. Qi and S.-C. Zhang, *Rev. Mod. Phys.* **83**, 1057 (2011).
- [35] C.-K. Chiu, J. C. Y. Teo, A. P. Schnyder, and S. Ryu, *Rev. Mod. Phys.* **88**, 035005 (2016).
- [36] X.-G. Wen, *Rev. Mod. Phys.* **89**, 041004 (2017).
- [37] F. Liu, R. Lundgren, J. B. Curtis, P. Titum, J. R. Garrison, and A. V. Gorshkov, arXiv e-prints, arXiv:1902.10720 (2019), [arXiv:1902.10720 \[quant-ph\]](https://arxiv.org/abs/1902.10720).
- [38] A. Y. Kitaev, *Physics-Uspekhi* **44**, 131 (2001).
- [39] M. Heyl, A. Polkovnikov, and S. Kehrein, *Phys. Rev. Lett.* **110**, 135704 (2013).
- [40] S. Vajna and B. Dóra, *Phys. Rev. B* **91**, 155127 (2015).
- [41] J. C. Budich and M. Heyl, *Phys. Rev. B* **93**, 085416 (2016).
- [42] S. Sharma, U. Divakaran, A. Polkovnikov, and A. Dutta, *Phys. Rev. B* **93**, 144306 (2016).
- [43] U. Bhattacharya and A. Dutta, *Phys. Rev. B* **96**, 014302 (2017).
- [44] C. Wang, P. Zhang, X. Chen, J. Yu, and H. Zhai, *Phys. Rev. Lett.* **118**, 185701 (2017).
- [45] J. Yu, *Phys. Rev. A* **96**, 023601 (2017).
- [46] J. Lang, B. Frank, and J. C. Halimeh, *Phys. Rev. Lett.* **121**, 130603 (2018).
- [47] L. Zhang, L. Zhang, S. Niu, and X.-J. Liu, *Science Bulletin* **63**, 1385 (2018).
- [48] M. Heyl, *Reports on Progress in Physics* **81**, 054001 (2018).
- [49] B. Žunkovič, M. Heyl, M. Knap, and A. Silva, *Phys. Rev. Lett.* **120**, 130601 (2018).
- [50] X. Qiu, T.-S. Deng, G.-C. Guo, and W. Yi, *Phys. Rev. A* **98**, 021601 (2018).
- [51] P.-Y. Chang, *Phys. Rev. B* **97**, 224304 (2018).
- [52] M. Ezawa, *Phys. Rev. B* **98**, 205406 (2018).
- [53] Z. Gong and M. Ueda, *Phys. Rev. Lett.* **121**, 250601 (2018).
- [54] P. Jurcevic, H. Shen, P. Hauke, C. Maier, T. Brydges, C. Hempel, B. P. Lanyon, M. Heyl, R. Blatt, and C. F. Roos, *Phys. Rev. Lett.* **119**, 080501 (2017).
- [55] N. Fläschner, D. Vogel, M. Tarnowski, B. Rem, D.-S. Lühmann, M. Heyl, J. Budich, L. Mathey, K. Sengstock, and C. Weitenberg, *Nature Physics* **14**, 265 (2018).
- [56] M. Tarnowski, F. N. Ünal, N. Fläschner, B. S. Rem, A. Eckardt, K. Sengstock, and C. Weitenberg, *Nature communications* **10**, 1728 (2019).
- [57] W. Sun, C.-R. Yi, B.-Z. Wang, W.-W. Zhang, B. C. Sanders, X.-T. Xu, Z.-Y. Wang, J. Schmiedmayer, Y. Deng, X.-J. Liu, S. Chen, and J.-W. Pan, *Phys. Rev. Lett.* **121**, 250403 (2018).
- [58] C.-R. Yi, L. Zhang, L. Zhang, R.-H. Jiao, X.-C. Cheng, Z.-Y. Wang, X.-T. Xu, W. Sun, X.-J. Liu, and S. Chen, arXiv e-prints, arXiv:1905.06478 (2019), [arXiv:1905.06478 \[cond-mat.quant-gas\]](https://arxiv.org/abs/1905.06478).
- [59] A. P. Schnyder, S. Ryu, A. Furusaki, and A. W. W. Ludwig, *Phys. Rev. B* **78**, 195125 (2008).
- [60] A. Kitaev, in *AIP Conference Proceedings*, Vol. 1134 (AIP, 2009) pp. 22–30.
- [61] S. Ryu, A. Schnyder, A. Furusaki, and A. Ludwig, *New J. Phys.* **12**, 065010 (2010).
- [62] See details in appendices.
- [63] A. R. Brown and L. Susskind, *Phys. Rev. D* **100**, 046020 (2019).
- [64] M. D. Caio, N. R. Cooper, and M. J. Bhaseen, *Phys. Rev. Lett.* **115**, 236403 (2015).
- [65] L. D'Alessio and M. Rigol, *Nature communications* **6**, 8336 (2015).
- [66] D. W. F. Alves and G. Camilo, *Journal of High Energy Physics* **2018**, 29 (2018).
- [67] J. Jiang, J. Shan, and J. Yang, arXiv e-prints, arXiv:1810.00537 (2018), [arXiv:1810.00537 \[hep-th\]](https://arxiv.org/abs/1810.00537).
- [68] Z.-Y. Fan and M. Guo, *Nuclear Physics B*, 114818 (2019).
- [69] T. Ali, A. Bhattacharyya, S. Shajidul Haque, E. H. Kim, and N. Moynihan, arXiv e-prints, arXiv:1811.05985 (2018),

- [arXiv:1811.05985 \[hep-th\]](#).
- [70] T. Ali, A. Bhattacharyya, S. S. Haque, E. H. Kim, and N. Moynihan, *Journal of High Energy Physics* **2019**, 87 (2019), [arXiv:1810.02734 \[hep-th\]](#).
- [71] M. Moosa, *Journal of High Energy Physics* **2018**, 31 (2018).
- [72] H. A. Camargo, P. Caputa, D. Das, M. P. Heller, and R. Jefferson, *Phys. Rev. Lett.* **122**, 081601 (2019).
- [73] D. S. Ageev, arXiv e-prints , [arXiv:1902.03632 \(2019\)](#), [arXiv:1902.03632 \[hep-th\]](#).
- [74] P. Roushan, C. Neill, Y. Chen, M. Kolodrubetz, C. Quintana, N. Leung, M. Fang, R. Barends, B. Campbell, Z. Chen, B. Chiaro, A. Dunsworth, E. Jeffrey, J. Kelly, A. Megrant, J. Mutus, P. J. J. O'Malley, D. Sank, A. Vainsencher, J. Wenner, T. White, A. Polkovnikov, A. N. Cleland, and J. M. Martinis, *Nature* **515**, 241 (2014).